ADVANCES IN MODELING COLLISIONS ON ICY BODIES. S. T. Stewart and L. E. Senft. Department of Earth and Planetary Sciences, Harvard University, 20 Oxford Street, Cambridge, MA 02138 (sstewart@eps.harvard.edu).

Introduction: Impact cratering is one of the major geologic processes on the icy planets and satellites in the outer solar system. The outcome of impact calculations have been used to suggest the presence of transient liquid water after cratering events [1-4] and to infer the thickness of brittle crusts [5]. These studies rely heavily on the accuracy of (1) the model equation of state of H_2O to infer the post-impact temperature field and the occurrence of phase changes and (2) the constitutive model to describe the shear and tensile strengths and the degradation of strength with damage. Here, we summarize recent advances in the quality of equation of state and constitutive models for H_2O and implications for collisional processes on icy bodies.

Equation of State Models: Because of the complexity of the H_2O phase diagram, most equation of state (EOS) models used in hydrocode calculations have been tailored to specific phases with little or no ability to extend calculations to broad regions of the phase diagram. In general the phase diagram is simplified, with one solid phase, liquid, and vapor (with simplified dissociation). Recent development includes an ANEOS-based multiphase equation of state that includes all of the stable solid phases [6].

We have developed a new tabular equation of state for H_2O [7]. The table includes three solid phases (ices Ih, VI, and VII), liquid, and vapor. The EOS of the phases and phase boundaries are experimentally determined. The liquid and vapor are described by the International Association for the Properties of Water and Steam (IAPWS) [8]. The equation of state of ice Ih is given by [9]. The equation of state of ices VI and VII are taken from [10], and the phase boundaries are given by [8, 11]. The model shock Hugoniots are compared with experimental Hugoniots in Fig. 1.

A crucial experimental data set that has been lacking for equation of state model validation is shock temperature measurements starting in the ice phase (shock temperatures in liquid water has been measured by [12, 13]). In the Shock Compression Laboratory at Harvard, we have new peak-shock and post-shock temperature measurements in polycrystalline ice Ih in the peak shock pressure range of 8 to 14 GPa [14]. Peak shock temperatures range from 650 to 1000 K.

The post-shock temperature provides direct information about the onset and kinetics of shock-induced phase changes. Upon release from shock pressures of 8 to 14 GPa, the continuum temperature of ice is 373 to 550 K.

Our tabular EOS is in excellent agreement with all of the shock and post-shock temperature data on liquid water and ice Ih.

Strength Model: The strength model describes the response of a material to deviatoric stresses; we develop new strength parameters for H_2O based on laboratory data. We use the strength model developed by [15] and implemented into the CTH shock physics code by [16]. In this model, shear strength is linearly degraded from an intact strength value (strength controlled by the creation of new fractures) to a fragmented (strength controlled by dry friction) value. A dimensionless scalar variable (damage) is introduced to track this degradation; damage ranges from zero (completely intact) to one (completely fragemented). Thus, shear strength is a function of damage, temperature, and pressure, and tensile strength is a function of damage.

Strength parameters are chosen by fitting to quasi-static laboratory test data. We use uniaxial compressive strength temperature dependence data from [18], friction data from [19], dynamic tensile strength data from [20], and triaxial shear strength data from [21]. Fig. 2 shows the shear strength data of intact (non-damaged) ice from [21] (circles) and the shear strength data of fragmented (damaged) ice from [19] (triangles). Note that the strength of ice has a strong temperature dependence. We fit a temperature degradation function to uniaxial compression data from [18] and use this to calculate the strengths at other temperatures. For example, the intact and damaged shear strength curves at 210 K are shown. The method outlined above assumes that the temperature dependence for uniaxial compressive strength is the same as the temperature dependence at higher pressures and that intact and fragmented ice have the same temperature dependences. In reality, this is not true; for instance, the coefficient of friction of ice is not significantly temperature dependent until very close to the melting point, and also depends upon a number of other neglected factors (such as strain rate).

Measurements of fresh complex craters on the icy satellites show that these craters are in general much shallower than their lunar counterparts [25, 26], which is expected as a result of the very low coefficient of friction of ice (~0.2 for cold ice, 77 K) as compared to rock (~0.6). It has been shown that icy layers can significantly shallow depth to diameter ratios [7, 27]. Furthermore, crater collapse may be aided by frictional melting processes [28]. At a temperature of -10° C, the coefficient of friction of ice approaches 0.001 as the sliding velocity along the fault approaches 1 m/s. Note that the friction coefficient also depends on temperature, but there is a lack of data for high sliding velocities and low temperatures; thus, it is unclear how much heating needs to occur for frictional melting to play a role in crater collapse on icy bodies. An alternative approach is to model crater collapse on icy bodies using acoustic fluidization [29].

Summary: We have developed a new multi-phase equation of state for water. We have also developed strength parameters to model ice over a wide range of conditions. With these advances, we are now able to model collisions throughout the solar system with much better accuracy.

References: [1] Artemieva, N. and J.I. Lunine (2005) *Icarus* **175**(2), 522-533. [2] Artemieva, N. and J. Lunine (2003) *Icarus* **164**(2), 471-480. [3] Pierazzo, E., N.A. Artemieva, and B.A. Ivanov (2005) *Geological Society of America Special Paper* **384**, 443-457. [4] Stewart, S.T., J.D. O'Keefe, and T.J. Ahrens (2004) *Shock Compression of Condensed Matter -- 2003*, American Institute of Physics: Melville, NY, p. 1484-1487. [5] Turtle, E.P. and E. Pierazzo (2001) *Science* **294**(5545), 1326-1328. [6] Ivanov, B.A. (2005) *LPSC* **36**, Abs. 1232. [7] Senft, L.E. and S.T. Stewart (submitted) *Meteoritics & Planetary Science*. [8] Wagner, W. and A. Pruss (2002) *Journal of Physical and Chemical Reference Data* **31**(2), 387-535. [9] Feistel, R. and W. Wagner (2006) *Journal of Physical and Chemical Reference Data* **35**(2), 1021-1047. [10] Stewart, S.T. and T.J. Ahrens (2005) *JGR* **110**, E03005. [11] Frank, M.R., Y.W. Fei, and J.Z. Hu (2004) *Geochimica et Cosmochimica Acta* **68**(13), 2781-2790. [12] Kormer, S.B. (1968) *Soviet Physics USPEKHI* **11**(2), 229-254. [13] Lyzenga, G.A., et al. (1982) *Journal of Chemical Physics* **76**(12), 6282-6286. [14] Stewart, S.T., A. Seifter, and A.W. Obst (2008) *LPSC* **39**, Abs. 2301. [15] Collins, G.S., H.J. Melosh, and B.A. Ivanov (2004) *Meteoritics and Planetary Science* **39**(2), 217-231. [16] Senft, L.E. and S.T. Stewart (2007) *Journal of Geophysical Research* **112**(E11), doi: 10.1029/2007JE002894. [17] Cohn, S.N. and T.J. Ahrens (1981) *Journal of Geophysical Research* **86**(B3), 1794-1802. [18] Arakawa, M. and N. Maeno (1997) *Cold Regions Science and Technology* **26**, 215-229. [19] Beeman, M., W.B. Durham, and S.H. Kirby (1988) *Journal of Geophysical Research* **93**(B7), 7625-7633. [20] Lange, M.A. and T.J. Ahrens (1983) *Journal of Geophysical Research* **88**(B2), 1197-1208. [21] Sammonds, P.R., S.A.F. Murrell, and M.A. Rist (1998) *Journal of Geophysical Research* **103**(C10), 21,795-21,816. [22] Griffith, A.A. (1920) *Philosophical Transactions of the Royal Society of London A* **34**, 137-154. [23] Housen, K.R. and K.A. Holsapple (1990) *Icarus* **84**, 226-253. [24] Housen, K.R. and K.A. Holsapple (1999) *Icarus* **142**, 21-23. [25] Schenk, P.M. (2002) *Nature* **417**, 419-421. [26] Schenk, P.M. (2007) *Ices, Oceans, and Fire: Satellite of the Outer Solar System Conference*, Abs. 6025 [27] Senft, L.E. and S. T. Stewart (2007) *Workshop on Impact Cratering II*, Abs. 8008 [28] Senft, L.E. and S. T. Stewart (2008) *LPSC* **39**, Abs. 1417 [29] Bray, V.J., G.S. Collins, J.V. Morgan, and P.M Schenk (2007) *Workshop on Impact Crater II*, Abs. 8056.

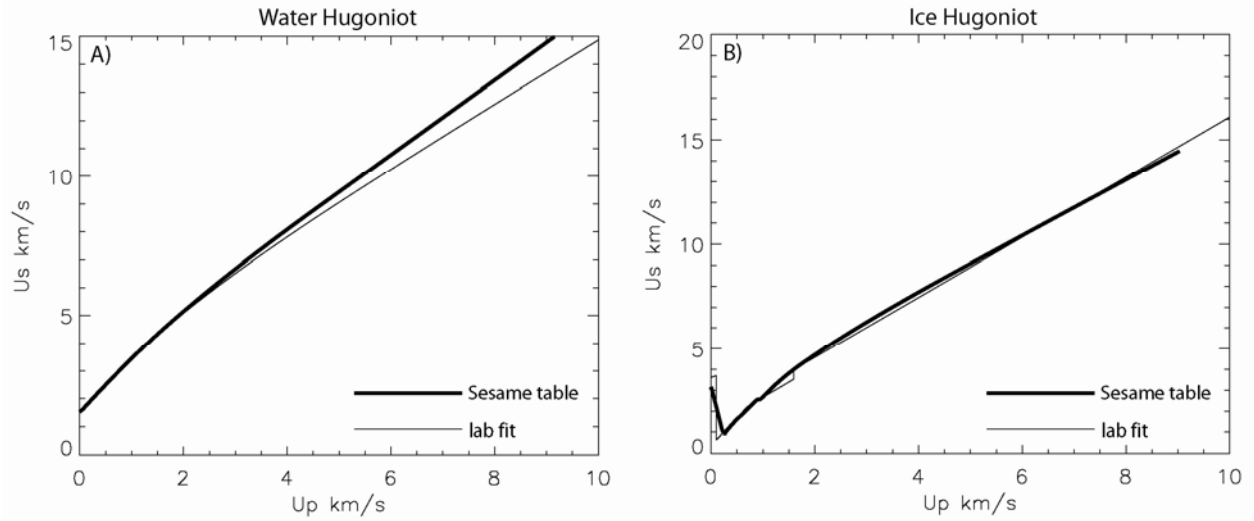

Fig. 1. Hugoniots for water (A; initial temperature of 300 K) and ice (B; initial temperature of 250-263 K) calculated from our Sesame table for H_2O (thick lines) compared to lab hugoniots (thin lines) from [10]. U_s is shock velocity, U_p is particle velocity.

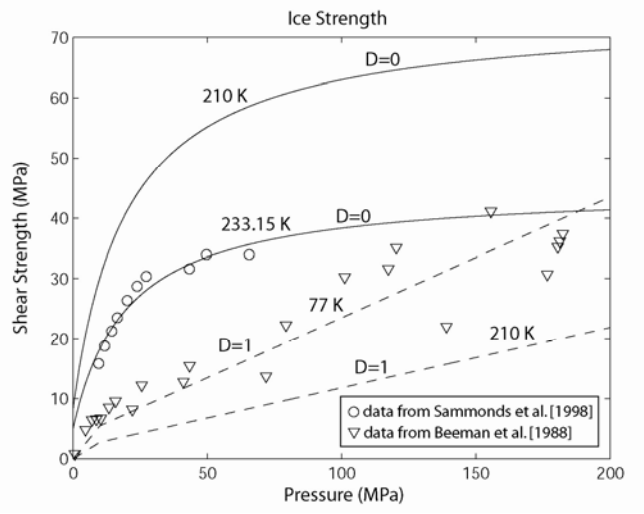

Fig. 2. Shear strength (in terms of the square root of the second invariant of the deviatoric stress tensor, $\sqrt{J_2}$) for fragmented ice (i.e. ice-on-ice friction; dashed lines) and intact ice (solid lines). Circles are data at 233.15 K from [21], and triangles are data at 77 K from [19]. Also shown are strength curves at 210 K, appropriate for models of cratering on Mars.